EFDA–JET–PR(12)17

B. Baiocchi, P.Mantica, C. Giroud, T. Johnson, V. Naulin, A. Salmi,
T. Tala, M.Tsalas and JET EFDA contributors

Discriminating the Role of Rotation and its Gradient in Determining Ion Stiffness Mitigation in JET

Discriminating the Role of Rotation and its Gradient in Determining Ion Stiffness Mitigation in JET

B. Baiocchi[1,2], P.Mantica[2], C. Giroud[3], T. Johnson[4], V. Naulin[5], A. Salmi[6], T. Tala[7], M.Tsalas[8] and JET EFDA contributors*

JET-EFDA, Culham Science Centre, OX14 3DB, Abingdon, UK

[1]Università degliStudi di Milano, Milano, Italy
[2]Istituto di Fisica del Plasma 'P.Caldirola', AssociazioneEuratom-ENEA-CNR, Milano, Italy
[3]EURATOM-CCFE Fusion Association, Culham Science Centre, OX14 3DB, Abingdon, OXON, UK
[4]Association EURATOM - VR, Fusion Plasma Physics, EES, KTH, Stockholm, Sweden
[5]Association Euratom-Risø DTU, DK-4000 Roskilde, Denmark
[6]Association EURATOM-Tekes, Aalto University, Department of Applied Physics, Finland
[7]Association EURATOM-Tekes, VTT, P.O. Box 1000, FIN-02044 VTT, Finland
[8]FOM Institute DIFFER, Association EURATOM-FOM, Nieuwegein, the Netherlands
** See annex of F. Romanelli et al, "Overview of JET Results",*
(23rd IAEA Fusion Energy Conference, Daejon, Republic of Korea (2010)).

Preprint of Paper to be submitted for publication in
Plasma Physics and Controlled Fusion

ABSTRACT

Starting from recent JET experimental results that show a significant reduction of ion stiffness in the plasma core region due to plasma rotation in presence of low magnetic shear, an experiment was carried out at JET in order to separate the role of rotation and rotation gradient in mitigating the ion stiffness level. Enhanced toroidal field ripple (up to 1.5%) and external resonant magnetic fields are the two mechanisms used to try and decouple the rotation value from its gradient. In addition, shots with reversed toroidal field and plasma current, yielding counter-current neutral beam injection, were compared to standard co-injection cases. These tools also allowed varying the rotation independently of the injected power. Shots with high rotation gradient have been found to maintain their low stiffness level even when the absolute value of the rotation was significantly reduced. Conversely, high but flat rotation yields much less peaked ion temperature profiles than a peaked rotation profile with lower values. This behaviour suggests the rotation gradient as the main player in reducing the ion stiffness level. In addition, it has been found that inverting the rotation gradient sign does not suppress its effect on ion stiffness.

1. INTRODUCTION

Theoretical models describe turbulent ion heat transport as mainly driven by Ion Temperature Gradient (ITG) modes. They become unstable above a threshold value of the inverse ion temperature (T_i) gradient length (R/L_{Ti}, where R is the tokamak major radius and $L_{Ti} := T_i/\mathrm{grad}T_i$) and lead the ion heat flux to increase strongly with R/L_{Ti}, thereby preventing attaining R/L_{Ti} values much higher than the threshold value. This behaviour can be described by the stiffness level, a parameter that quantifies the tendency of the T_i profiles to remain tied to the threshold independently of the amount of heating power applied. The description of turbulent ion heat transport in terms of threshold and stiffness has been proposed theoretically [1-3] and supported by experimental observations [4-8]. Knowing the dependence of threshold and stiffness on plasma physical quantities is then relevant to investigate how the ion heat transport and then the plasma performances can be acted upon.

Parametric studies about the role of T_e/T_i, q profile, magnetic shear and toroidal rotation (Ω) have been carried out through experimental investigations in the JET tokamak [5]. In particular the toroidal rotation in presence of low magnetic shear, as described in [4,7], has been found to have a significant effect of reduction of ion stiffness, yielding much higher R/L_{Ti} than due to the mere $\Omega_{E\times B}$ threshold up-shift [9]. However in the experiments reported in [7], the values of rotation and of its gradient were correlated, so it was not clear if the effect of reducing the stiffness had to be ascribed to Ω or $\nabla\Omega$.

An experiment was then carried out in JET in order to decouple the effect of Ω and $\nabla\Omega$. Two methods of plasma rotation braking have been used. The first one is based on enhancing the toroidal field (B_T) ripple. In tokamaks the B_T ripple, a toroidally periodic variation of the external B_T, exists because of the finite number of B_T coils. JET has the possibility of varying the ripple amplitude [10]. This was found to have significant effects on the plasma rotation [11], since a large B_T ripple by breaking the axi-symmetry of the magnetic field induces enhanced non-ambipolar particle losses.

This takes place particularly in the external region of the plasma and leads to an edge counter-current torque that brakes the plasma rotation. The second method consists in the application of low n external magnetic perturbation fields produced by the set of four external Error Field Correction Coils (EFCC) of JET [12]. Also in this case previous experiments showed strong effects on the plasma rotation due to breaking the toroidal symmetry and slowing down the plasma rotation by Neoclassical Toroidal Viscosity [13]. Applying these techniques, besides providing to a certain extent a decoupling of Ω and $\nabla\Omega$, allows in addition to perform discharges with different rotation but constant total injected power, allowing to assess the effect of rotation on stiffness when rotation is decoupled from power. In [7], instead, lower values of rotation were obtained using less Neutral Beam Injection (NBI) power, apart from the case of reverse B_T shots with counter-NBI, which is also a remarkable method of decoupling rotation from its gradient and also from power, and will also be considered in this paper.

The experiment description and the obtained results are presented in section 2. From these, the conclusion is derived that the ion stiffness reduction has to be ascribed to rotation gradient rather than to rotation. In section 3 we show in addition that also a rotation gradient with reversed sign (hollow rotation) also acts mitigating stiffness. In section 4 the conclusions are reported.

2. ROTATION BRAKING EXPERIMENT

2.1 EXPERIMENTAL SET-UP

At JET it is possible to vary the B_T ripple amplitude δ, defined as $\delta = (B_{Tmax}-B_{Tmin})/(B_{Tmax}+B_{Tmin})$. For standard JET operations, that are carried out with a set of 32 B_T coils carrying equal current, $\delta = 0.08\%$. Because odd and even coils are powered independently, the imbalance current between the two coils sets can be changed increasing the B_T ripple up to $\delta = 3\%$. These values refer to the maximum B_T ripple values in the plasma, taken at the outer mid-plane at $R = 3.8$m and $z = 0$. Energetic particles can be toroidally trapped in the magnetic ripple and then drifted out of the plasma because of the field curvature. In addition the trajectory of banana-orbits trapped particles can be altered by B_T ripple, that causes them to drift radially outwards. In the presence of a large B_T ripple other ion losses, possibly those of thermal ions, may be involved [18]. The friction between circulating particles and those locally trapped in B_T ripple tends to reduce the toroidal rotation [19]. However the dominant effect on the toroidal rotation is given by the outward lost ion flow, that induces a radial return current j in order to preserve neutrality. The resulting j×B torque is always in the counter-current direction. It leads to a significant reduction of both the edge and core rotation, but affects less the core spatial gradient [20,10,11,21].

Also the external perturbation fields applied through the EFCC system influence the JET plasma rotation and rotation shear. The EFCC set consists of four square shaped coils mounted outside the vacuum vessel. Depending of the wiring of the EFCCs either $n = 1$ or $n = 2$ fields can be created. Low n perturbation fields break the toroidal symmetry. The plasma flows then along distorted flux surfaces and it is subjected to a drag toroidal force, due to the Neoclassical Toroidal Viscosity (NTV), that influences the plasma rotation and its gradient [22,23]. A reduction in toroidal rotation

at different radii by a same factor ($grad v_\phi / v_\phi$ = constant) has been observed over the whole plasma core and stronger rotation braking has been found near the edge pedestal [24, 12, 25].

The rotation braking experiments are performed in H-mode plasmas at $B_T = 2T$ for shots with varying B_T ripple and at $B_T = 1.85T$ for shots with EFCC, with $I_p = 1.5MA$, low triangularity, $q_{95} = \sim 5$, $n_{e0} \sim 3\ 10^{19}\ m^{-3}$, $0.9 < T_e/T_i < 1.1$. Ion Cyclotron Resonance Heating (ICRH) and NBI have been used as heating systems. Keeping the total injected power fixed, the ICRH and NBI powers have been varied to obtain a sufficiently wide ion heat flux scan and to observe different rotation profiles. In order to perform two basic steps of core ion heat flux scan, ICRH (0-2 MW) has been applied varying deposition between on- and off-axis at $\rho_{tor} \sim 0.7$. It has been used in a (H)-D scheme (33MHz on-axis, 42MHz off-axis) with $n_H/n_e \sim 8\%$ and 20-30% of the ICRH core power delivered to thermal ions. ICRH power deposition profiles have been obtained by the PION code [14] calculations, for NBI power deposition a first analysis has been done using the code PENCIL [15]. This code is computationally faster, however it omits the ion orbit physics and doesn't take into account the ripple effect. Then three representative discharges (one with enhanced BT ripple, one with standard ripple and one with the application of EFCCs fields) have been reprocessed with ASCOT [16], an orbit-following Monte Carlo code that includes in the calculations fast ion losses due to the enhanced B_T ripple [17]. The ripple effect has been found negligible for $\rho_{tor} < 0.4$, allowing to calculate the NBI heat fluxin the core – which is what is required for the stiffness study - without any ripple correction. However, the NBI ion heat flux obtained by ASCOT has been found 20% higher than that provided by the PENCIL code, with the same multiplication factor between the two code calculations for all the discharges. Since ASCOT features a more refined treatment of NBI deposition, the PENCIL NBI ion heat fluxes obtained for all shots have then been corrected by this multiplication factor, in order to minimize the systematic error. Different NBI powers from 4 to 7MW have been injected in the plasma to produce a large spectrum of high rotation profiles at standard ripple. For each case, enhanced B_T ripple or EFCCs have then been applied.

2.2 DATA ANALYSIS AND EXPERIMENTAL RESULTS

In Fig.1 the rotation as a function of the rotation gradient is shown for the investigated shots. Triangles refer to standard B_T ripple (0.08%) discharges, squares and diamonds to enhanced BT ripple discharges (respectively 1% and 1.5%) and EFCCs shots are indicated by circles. The values of rotation, measured by means of Charge eXchange Recombination Spectroscopy (CXRS), have been averaged in time over a stationary interval and taken at the radial position $\rho_{tor} = 0.25$: it encloses the on-axis power but not the off-axis one, giving the maximum ion heat flux scan, useful in order to investigate the stiffness level of the analysed shots. The gradient of rotation has been calculated from the channels 2-5 of the CX diagnostic, with centre at $\rho_{tor} = 0.25$.

Discharges without methods of rotation braking present higher values of rotation and rotation gradient with respect to discharges in which enhanced B_T ripple or EFCCs have been applied. The enhanced B_T ripple shots reach higher values of rotation gradient relative to the rotation value if compared with the trend proper of the standard B_T discharges. Shots where EFCCs are switched on

are in line with the standard discharge trend. Only enhanced B_T ripple seems to be able to decouple rotation and rotation gradient for discharges characterized by the above reported physical values and with the above described heating powers. It is then possible to investigate the role that rotation and rotation gradient have separately on the ion stiffness.

To this aim, a first analysis has been done by comparing T_i profiles of plasmas characterized by similar gradients of rotation and different rotation values, as in the example shown in Fig.2. It refers to one of the shots with enhanced B_T ripple characterized by reduced rotation with respect to rotation gradient and a standard B_T ripple shot with similar power level and ion heat deposition and plasma parameters except for the ripple level, with a similar rotation gradient but larger rotation value all along the plasma radius. As shown in Fig.2b, the T_i profiles for the two shots and their gradients are identical, even if the values of rotation differ significantly. This is verified not only around the radial position $\rho_{tor} = 0.25$ but along all the temperature profiles (the perfect match of the two profiles has to be considered a coincidence).

The method of enhancing the B_T ripple or applying the EFCCs fields does not allow to obtain discharges with a reduced rotation gradient with respect to rotation value. Therefore, limiting the analysis to shots of this braking experiment, a comparison between plasmas with similar values of rotation and different rotation gradient would not be feasible. However, using as auxiliary heating counter-NBI in reverse B_T and I_p configuration is known to produce plasmas with flatter toroidal rotation with respect to the corresponding co-NBI plasmas because of off-axis torque deposition [7, 26]. A discharge that belongs to such set of experiments (the Pulse No: 59630 at 14s), characterized by similar parameters and standard BT ripple and heated by counter-NBI with a power level nearly equal to the shots of the rotation braking experiments, was then taken into account for the comparison. In Fig.3 it is compared with an enhanced ripple discharge, which has similar values of rotation and higher rotation gradient around the radial position $\rho_{tor} = 0.25$ (Fig.3a). The associated T_i profiles shown in Fig.3b are then very different, indicating that the similar absolute value of Ω does not lead to similar core T_i peaking if $\nabla\Omega$ is very different. As we can see in Fig.3c, although the power deposition profiles are different for the two discharges (in the case of counter-NBI the distribution of power to ions and electrons is less peaked in the central part of the plasma), inside the considered radius $\rho_{tor} = 0.25$ the counter-NBI shot does not have significantly less ion power than the co-NBI shot (3.8MW against 4.1, see also [7], where an exhaustive analysis about the comparison between co- and counter-NBI plasmas is reported). On the contrary, in terms of normalized ion heat flux, one can see in Fig.4 that the counter-NBi shot is the one with the highest normalized ion heat flux.

We conclude that from the simple comparison of experimental profiles, the Ti profile peaking seems related more to $\nabla\Omega$ than to Ω.

One important limitation of simple profile analysis is that it cannot determine if larger ∇T_i are due to higher ion threshold values or to lower ion stiffness values. In order to clarify this point a second type of analysis has been done, taking into account the value of the ion heat flux in all the discharges. Although this point was already clarified in [7], a further confirmation was searched in this set of discharges, where in addition we try to separate the different roles of $\nabla\Omega$ and Ω.

The ion heat fluxes q_i at the radial position $\rho_{tor} = 0.25$ are plotted in Fig.4 as functions of the logarithmic gradient of the ion temperature R/L_{Ti} calculated at the same radius. As in [7], q_i is calculated by spatial integration of ion power density profiles and by determining the collisional electron-ion transfer by means of interpretative transport simulations. The heat flux is expressed in gyro-Bohm units. Gyro-Bohm scaling has been predicted to characterize plasmas dominated by anomalous transport [2]. In the following formula the gyro-Bohm normalization is made explicit

$$q_i^{GB} = \frac{q_i}{(\rho/R)^2 v_{ith} n_i T_i} \quad (1)$$

where ρ_i is the ion Larmor radius, R is the major radius of the JET tokamak, $v_{ith} = \sqrt{(T_i/m_i)}$, n_i the ion density and T_i the ion temperature. R/L_{Ti} is obtained by an exponential best-fit over 4 CX channels, with centre in $\rho_{tor} = 0.25$ and averaged in time over a stationary interval. The ion temperature gradient is calculated with respect to the flux surface minor radius, $\rho = (R_{out}-R_{in})/2$, where R_{out} (R_{in}) is the outer (inner) boundary of the flux surface on the magnetic axis plane. In Fig.4 circles and squares represent pulses characterized by coupled rotation and rotation gradient values: circles are low rotation shots with $\nabla\Omega<24$ krad/ms and $\Omega<25$ krad/s; squares are high rotation shots with $\nabla\Omega>24$ krad/ms and $\Omega>25$ krad/s. The two sets of points form two distinct curves: the one formed by circular points is characterized by high stiffness level, and the one formed by square points is characterized by low stiffness. We can see that the behaviour shown by the experimental results described in [7] is confirmed. Points with decoupled rotation gradient and rotation are shown with reversed triangles. They are characterized by $\nabla\Omega>24$ krad/ms and $\Omega<25$ krad/s. These points sit well in low stiffness curve, although they are characterized by low rotation values. Then we can conclude that is the rotation gradient that matters in reducing the ion stiffness level, and not the absolute value of rotation. With respect to the results represented in [7] in this experiment the excursion of q_i^{GB} and R/L_{Ti} has been limited by the impossibility of using ^{3}He ion heating due to absence of suitable ICRH frequencies at the low B_T values needed for enhanced ripple. Therefore the highest values of R/L_{Ti} are not achievable in the enhanced ripple discharges. Also very low qi values, which would be relevant for the determination of the ion threshold, are not feasible because they require off-axis ICRH, which is too risky in conditions of high B_T ripple due to losses of highly energetic ICRH ions in the plasma periphery.

3. RF DRIVEN HOLLOW ROTATION EXPERIMENT

The discharges of the above described experiment and those belonging to the experiments reported in [7] are characterized by profiles of plasma toroidal rotation that are monotonic and peaked in the central part of the plasma, i. e. with negative rotation gradient. In order to understand if the sign of the rotation gradient can play a role in influencing the ion stiffness, and then the ion temperature profiles, discharges belonging to a different experiment also based on the use of (^{3}He)-D ICRH have been analysed. Some experimental observations on JET and C-MOD have shown that the toroidal rotation is sensitive to the ^{3}He concentration [27-29]. In particular in some range of concentrations

ICRF mode conversion has been found to drive toroidal flow in the co-I_p direction in C-MOD whilst in JET it gives origin to hollow rotation profiles, leading to suppose the existence of a torque in the counter-I_p direction [30]. A selection of discharges that exhibit hollow rotation profiles in presence of (^{3}He)-D ICRH heating have been analysed and compared with similar discharges in which the rotation profile was not hollow but flat.

3.1 EXPERIMENTAL SET-UP

The analysis refers to L-mode plasmas, characterized by $B_T = 3.3T$, $I_P = 1.8MA$, $n_{e0} = 3.5\times10^{19}$ m^{-3}. The heating is provided by RF power, with a frequency of 33MHz and a power of 7MW. The power deposition has been varied from dominant electron in 3% (H)-D minority to dominant ion in 4-8% (^{3}He)-D to dominant electron in 20% (^{3}He)-D where mode conversion takes place. Other discharges characterized by the parameters reported above but NBI heated have been included in our analysis, in order to have high negative rotation gradient plasmas to compare with the positive ones obtained from hollow rotation profiles. The power deposition and then the ion heat flux have been derived using the codes PION and ASCOT. Physical quantities have been measured and obtained as described in the previous section.

3.2 DATA ANALYSIS AND EXPERIMENTAL RESULTS

In Fig.5 rotation profiles and corresponding T_i profiles of one pulse at two different times (and different ^{3}He concentration) are shown. The rotation profile is hollow for $\rho_{torr}<0.3$ at $t = 7.5s$, with rotation values still in the co-I_p direction. The rotation becomes flat at t=11.2 s. As shown in Fig.5b, we find different T_i profiles in the plasma region within $\rho_{tor} = 0.3$. In this zone higher values of the T_i gradient are observed for the case of hollow rotation where the rotation gradient is rather high and positive, even if the rotation value is lower with respect to the case of flat rotation.

In order to compare properly the different shots, they have been plotted again in the q_i^{gB} versus R/L_{Ti} plot in Fig.6. Here circles, characterized by low Ω and $\nabla\Omega$, belong to the high stiffness curve, triangles have medium Ω and $\nabla\Omega$ and sit in the medium stiffness curve and squares, which are characterized by high Ω and $\nabla\Omega$, form the low stiffness curve, consistently with the graph of Fig.4. The points obtained from the profiles shown in Fig.5 are encircled. The one with flat rotation has a low value of Ω and $\nabla\Omega$, so it is shown with a circle. It is found to sit among the other circles and clearly belongs to high stiffness family. The point calculated at the time in which the rotation is hollow is represented by a reversed triangle and is characterized by medium positive $\nabla\Omega$ and low Ω. The normalized ion heat flux in the hollow rotation cases is comparable to that of other flat cases, whilst the ratio T_e/T_i is a bit higher in the case of hollow rotation, which should even decrease R/L_{Ti} in this case due to a threshold decrease [5]. Instead, a systematic high value of R/L_{Ti} is seen in hollow cases, which we ascribe to reduced stiffness due to the (positive) rotation gradient. We can see that the points with medium rotation gradient belong to the medium stiffness curve independently of the sign of the gradient. It is then the absolute value of the rotation gradient that influences the ion stiffness level, no matter what sign it has.

CONCLUSIONS

Experiments have been presented where the correlation between the absolute value of the rotation and its gradient has been broken by enhancing the B_T ripple, which has effect on the rotation, lowering its value, while it acts less strongly on the rotation gradient. The use of magnetic perturbations by EFCCs has not been as effective as B_T ripple in breaking the correlation.

Comparing pairs of discharges characterized by similar rotation value and different rotation gradient and pairs of discharges with similar rotation gradient and different rotation value, the observed behaviour of the ion temperature profiles indicates a dependence of the T_i peaking on the gradient of rotation rather than its value. In addition, the analysis of all the shots of the experiment in terms of the q_i^{GB} versus R/L_{Ti} plot has shown net distinct curves of different ion stiffness for different gradients of rotation, confirming the previous results of [7] also in conditions where rotation is varied at similar constant total power. In particular, the discharges with decoupled low rotation and high rotation gradient sit well in the low stiffness curve. We can then conclude that the ion stiffness mitigation is due to the rotation gradient rather than to the rotation value.

By comparing discharges characterized by hollow rotation profiles with discharges with flat rotation profiles, the Ti profile peaking is observed to be higher in the case of hollow rotation, i. e. for a high positive rotation gradient, although the rotation value is lower than in the cases with flat rotation profile. Placing these discharges in the q_i^{GB} versus R/L_{Ti} plot, in relation with discharges with lower values of rotation gradient and similar values but with opposite (negative) sign, results indicate that the level of ion stiffness depends on the absolute value of the rotation gradient, independently of its sign.

ACKNOWLEDGEMENT

This work, supported by the European Communities under the contract of Association EURATOM/ ENEA-CNR, was carried out within the framework of EFDA and under the JET-EFDA workprogramme [31]. The views and opinions expressed herein do not necessarily reflect those of the European Commission.

REFERENCES

[1]. Weiland J, 2000 "Collective Modes in Inhomogeneous Plasmas", Bristol: Institute of Physics Publishing.

[2]. Garbet X et al., 2004 Plasma Physics and Controlled Fusion **46** B557.

[3]. Guo S C and Romanelli F, 1993 Physics of Fluids **B5** 520.

[4]. Mantica P et al., 2011 Physical Review Letters **107** 135004.

[5]. Mantica P et al., 2011 Plasma Phys. Controlled Fusion **53** 124033.

[6]. Baker D R et al., 2001 Physics of Plasmas **10** 4419.

[7]. Mantica P et al., 2009 Physical Review Letters **102** 175002.

[8]. Ryter F et al., 2011 Nuclear Fusion **51** 113016.

[9]. Waltz R E et al., 1994 Physics of Plasmas **1** 2229.

[10]. Tubbing B et al., 1995 Proc. 22th EPS Conf. on Plasma Phys. Controlled Fusion(Montpellier, France, 1995) vol 19C p IV-001.
[11]. De Vries PC et al., 2008 Nuclear Fusion **48** 035007.
[12]. Barlow I et al., 2001 Fusion Engineering and Design **58-59** 189.
[13]. Liang Yet al., 2010 Nuclear Fusion **50** 025013.
[14]. Eriksson L-G, Hellsten T and Willen U, 1993 Nucl. Fusion **33** 1037.
[15]. Challis C D et al., 1989 Nuclear Fusion **29** 563.
[16]. Heikkinen J A and Sipilä S K, 1995 Physics of Plasmas **2** 3724.
[17]. Salmi A et al., 2011 Plasma Physics and Controlled Fusion **53** 085005.
[18]. Parail V et al., 2006 Proc. 21st Int. Conf. on Fusion Energy 2006 (Chengdu, China, 2006) (Vienna: IAEA) CD-ROM file TH/O8-5.
[19]. Mikhailovskii AB, 1995 Phys. Lett. A198 131.
[20]. Saibene G et al., 2008 Proc. 22nd Int. Conf. on Fusion Energy 2008 (Geneva, Switzerland, 2008) (Vienna: IAEA) CD-ROM file EX/2-1.
[21]. deVries PC et al., 2010 Plasma Phys. Controlled Fusion **52** 065004.
[22]. Liang Y et al., 2010 Nuclear Fusion **50** 025013.
[23]. Shaing KC, 2003 Physics of Plasmas **10** 1443.
[24]. Liang Y et al., 2007 Physical Review Letters **98** 265004.
[25]. Sun Y et al. 2010 Plasma Physics and Controlled Fusion **52** 105007.
[26]. deVries PC et al., 2008 Nuclear Fusion **48** 065006.
[27]. Lin Y et al., 2008 Physical Review Letters **101** 235002.
[28]. Eriksson LG et al., 2009 Plasma Physics and Controlled Fusion **51** 044008.
[29]. Tala T et al., 2010 Proceedings of the 23rd Int. Conf. on Fusion Energy 2010 (Dajeon, Korea, 2010) (Vienna: IAEA) CD-ROM file EXC/3-1 http://www-naweb.iaea.org/napc/physics/FEC/FEC2010/papers/exc_3-1.pdf
[30]. Lin Y et al., 2011 " ICRF mode conversion flow drive in D(^{3}He) plasmas on JET", accepted for publication in Plasma Physics and Controlled Fusion.
[31]. Romanelli F et al., 2010 Proceedings of the 23rd Int. Conf. on Fusion Energy 2010 (Dajeon, Korea, 2010) (Vienna: IAEA).

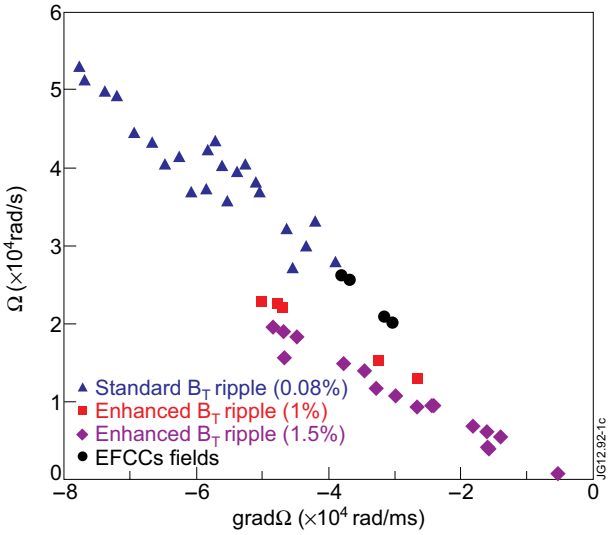

Figure 1: Toroidal rotation as a function of toroidal rotation gradient for standard B_T ripple (triangles), enhanced B_T ripple (squares 1% and diamonds 1.5%) and EFCCs (circles) shots. Rotation and its gradient have been taken at $\rho_{tor} = 0.25$.

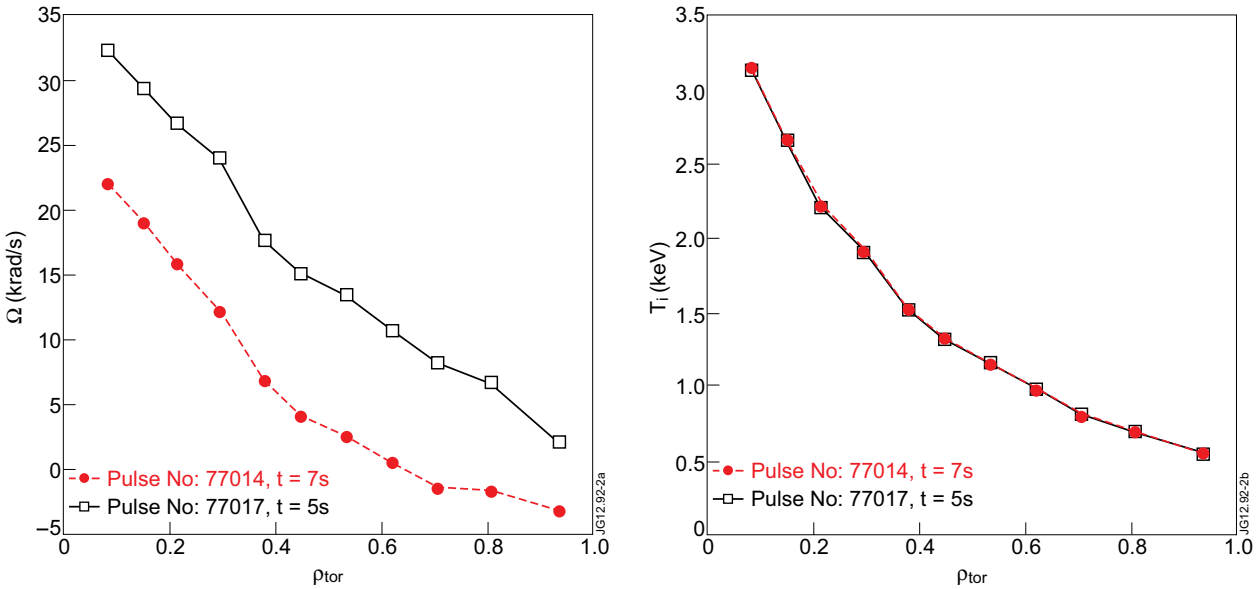

Figure 2: Toroidal rotation (a), ion temperature (b) profiles of two shots with standard (Pulse No: 77017, line with squares) and enhanced (Pulse No: 77014, line with circles) B_T ripple. In the neighbourhoods of $\rho_{tor} = 0.25$ the two shots are characterized by similar rotation gradient but significantly different rotation value. The profiles are taken at the times indicated in the legend of the graphs.

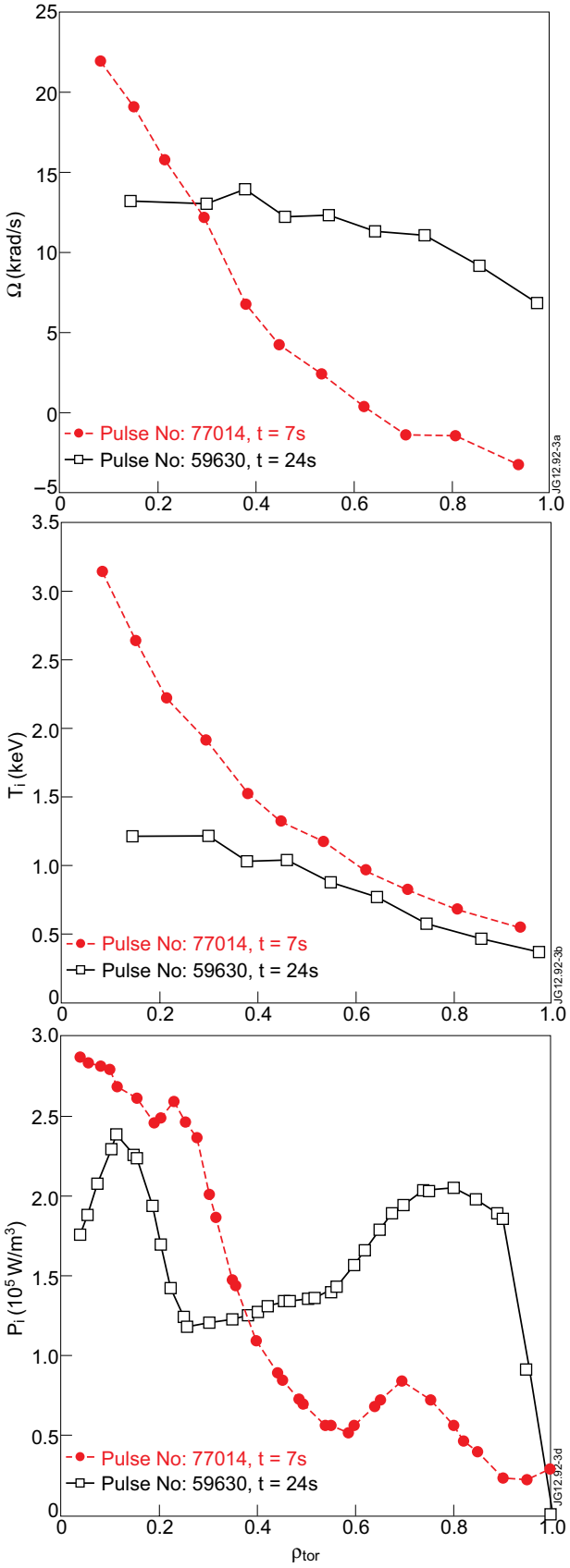

Figure 3: Toroidal rotation (a), relative ion temperature (b) and ion power deposition (c) profiles of one shot with enhanced BT ripple and co-NBI (Pulse No: 77014, solid line) and one shot with standard BT ripple and counter-NBI (Pulse No: 59630, dashed line). At $\rho_{tor} = 0.25$ Pulse No: 77014 is characterized by a value of rotation similar to the one of Pulse No: 59630 but very different gradient. The profiles are taken at the times indicated in the legend of the graphs.

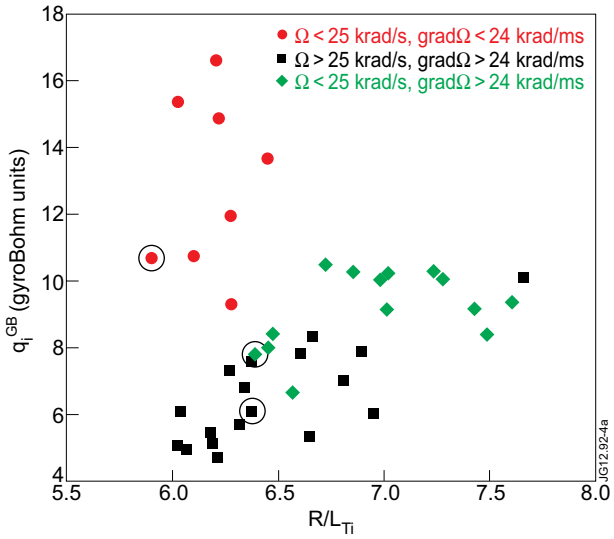

Figure 4: Gyro-Bohm normalized ion heat flux qi as a function of R/L_{Ti} at $\rho_{tor} = 0.25$. Points are grouped with respect to the values that $\nabla\Omega$ and Ω reach at $\rho_{tor} = 0.25$. Circled points refer to the shots treated in the first analysis in which temperature and rotation profiles have been compared. In particular Pulse No: 77014 is indicated by a square point, 77017 by a triangle and 59630 by a circle.

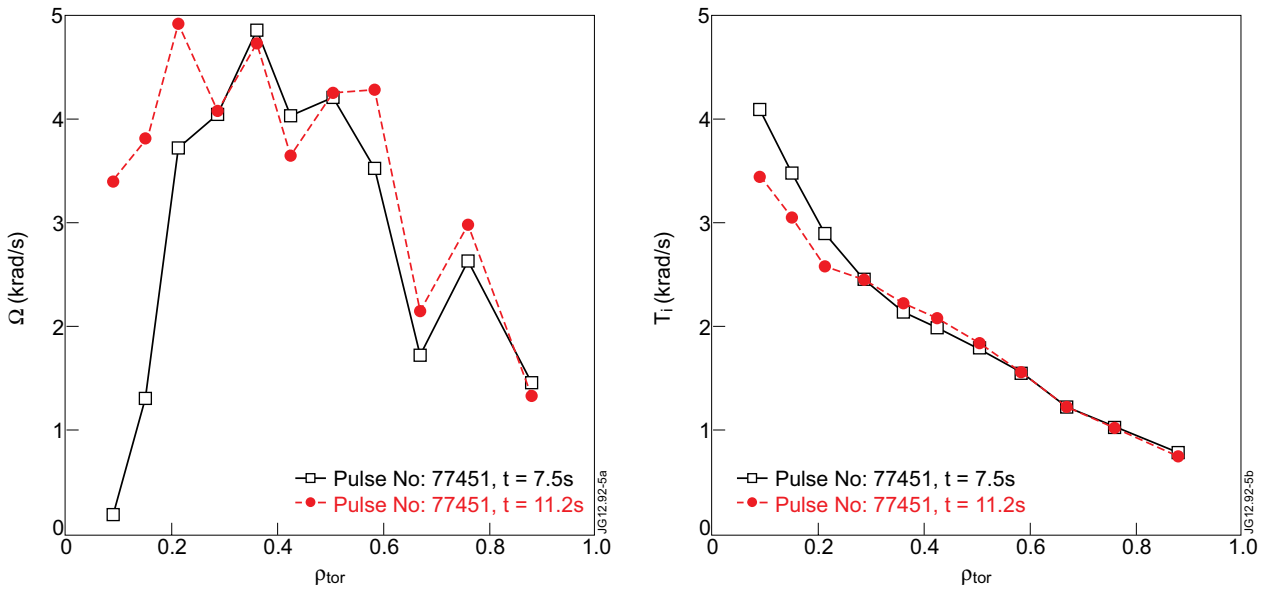

Figure 5: Toroidal rotation profiles (a) and relative ion temperature profiles (b) of Pulse No: 77451 at 7.5s and 11.2s. For $\rho_{tor}<0.3$ the Pulse No: 77451 at 7.5s (line with circles) is characterized by hollow rotation, instead at 11.2s (line with squares) the rotation is flat. In this region the T_i reaches higher values in the case with hollow rotation.

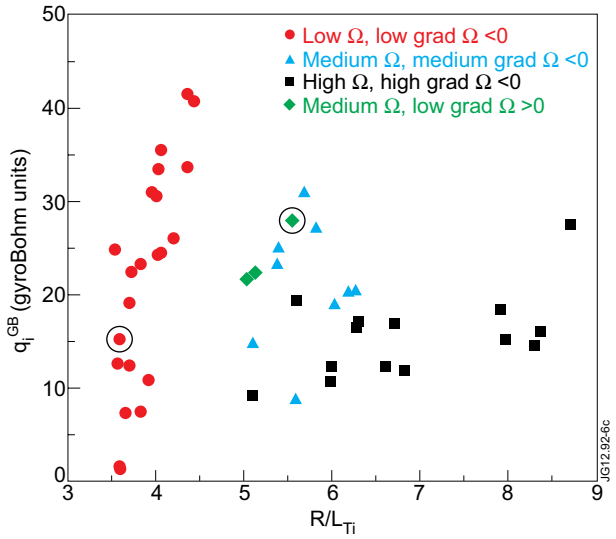

Figure 6: Gyro-Bohm normalized ion heat flux qi as a function of R/L_{Ti} at $\rho_{tor} = 0.25$. Points are grouped with respect to the values that $\nabla\Omega$ and Ω reach at $\rho_{tor} = 0.25$.